SYNTHESIS OF MAGNETITE NANOPARTICLES ON SUBSTRATE FOR WATER PURIFICATION

SYNOPSIS

of the thesis to be submitted for the partial fulfillment of the requirement for the degree of

DOCTOR OF PHILOSOPHY

in

Materials Science

by

SARITA
[Enrollment Number 126903]

DEPARTMENT OF PHYSICS & MATERIALS SCIENCE
JAYPEE UNIVERSITY OF INFORMATION TECHNOLOGY
WAKNAGHAT, SOLAN-173234, H.P., INDIA
FEBRUARY 2016

1. Introduction

Arsenic (As) a poisonous metalloid and a group 15 element is health wise dangerous contamination in both ground water as well as in surface water. It has become a serious issue worldwide due to its negative impacts on human health and environment [1-2]. Many parts of the world such as Bangladesh, India and countries in South and Southeast Asia have shown massive epidemics of arsenic poisoning [3-5]. Its exposure, even slightly higher than 0.1mg/L in drinking water, may cause neurological damage and its concentration reaching to 0.2mg/L creates the problem of dermatosis [6]. To avoid the problems caused by As contamination, the World Health Organization (WHO) and the United States Environmental Protection Agency (US EPA) have decreased its maximum concentration limit (MCL) from 50 to 10 μg/L [7].

Arsenic exists in the form of trivalent arsenite (as $H_3AsO_3^0$ and $H_2AsO_3^-$) and pentavalent arsenate (as $H_2AsO_4^-$ and $HAsO_4^{2-}$). The trivalent arsenite (As(III)) is 25 to 60 times more toxic than pentavalent arsenate (As(V)) and it is comparatively difficult to remove from water being non-ionic at natural water pH [8, 9]. Among various methods available for arsenic removal, iron based adsorption method proved to be more effective because both the As(III) and As(V) show strong affinity to iron bearing substances such as, magnetite (Fe_3O_4), zero valent iron-reduced graphite oxide, ferrihydrite, natural hematite and natural siderite [10-13]. If the iron based adsorbent is made in nano size it will enhance the adsorption performance due to higher surface area as compared with bulk counterpart.

However, despite of having advantages, the iron based nano sized adsorbents have some limitations, for example they need external magnetic field to be separated out from the water after use. A possible way to overcome the problem of requiring external magnetic field is that they can be used by making their filter cartridges but again this would be an expensive way since a large amount of the material would be needed in the cartridge. Therefore, the immobilization of the iron oxide nano powder on an inexpensive material such as the sand would be a better way to pave the method to a cost effective technology. Among the iron oxides, Fe_3O_4 shows high adsorption capacity and affinity [10, 14] to the As.

Here, we present a work to develop an inexpensive adsorbent by coating Fe_3O_4 nanoparticles on sand surface via co-precipitation method. The sand is used as a substrate for Fe_3O_4 to provide an economically feasible way for common man to get rid of the poisonous As from drinking water.

We have performed batch and column experiments to investigate the potential of synthesized adsorbent on As(III) and As(V) removal from water.

2. Objective of the work

The main objective of the work is to synthesize Fe_3O_4 nanoparticles on substrate for arsenic removal from drinking water.

3. Materials and methods

3.1. Materials

All the chemicals used in this study were of analytical grade, obtained from Sigma Aldrich. The chemicals were used as received without further purification. The solutions were prepared in Milli-Q water. Iron (III) chloride hexahydrate ($FeCl_3.6H_2O$), Iron (II) chloride ($FeCl_2$) and ammonia water (NH_4OH) were used for the synthesis of Fe_3O_4 nanoparticles. The substrate sand was procured from Beas River in Mandi district, Himachal Pradesh, India. The substrate (sand) was cleaned and etched by hydrochloric acid (HCl) and aquaregia (HNO_3 : HCl) solutions in 1:3 ratio, respectively before use. As(III) oxide and sodium arsenate dibasic heptahydrate ($HAsNa_2O_4.7H_2O$) were used as source of As(III) and As(V) respectively. The pH of arsenic solution was adjusted by standard 0.1 M HCl and 0.1 M NaOH, respectively. The co-ions (PO_4^{3-}, SO_4^{2-}, HCO_3^- and Cl^-) were produced in the solution by dissolving disodium hydrogen phosphate anhydrous (Na_2HPO_4), sodium sulphate (Na_2SO_4), sodium bicarbonate ($NaHCO_3$) and sodium chloride (NaCl) salts.

3.2. Coating of Fe_3O_4 nanoparticles on sand substrate

Initially, sand sieved to a geometric mean size of 0.6 to 0.9 mm was soaked in an acid solution (1.0M HCl) for 24 hours, which was then washed with distilled water several times and dried at 100^{o}C temperature. After cleaning, the sand was etched by using HNO_3 : HCl in a ratio 1:3 for 5 minutes and then it was rinsed in a stream of water to remove the etchant solution. Thus obtained sand was dispersed in a solution containing 2:1 ratio of $FeCl_3$ and $FeCl_2$, wherein NH_4OH solution was added drop wise at vigorous magnetic stirring keeping 70^{o}C temperature for 30 minutes under argon (Ar) gas flow. The addition of NH_4OH resulted in the co-precipitation reaction and thus the formation of Fe_3O_4 nanoparticles inside precursor solution.

Since the sand was present inside the precursor solution, the nucleation of Fe_3O_4 nanoparticles took place on the sand surface. Thus obtained mixture was aged at room temperature for 48 hours, which was then filtered and dried in a furnace at 85^oC using Ar gas environment. To ensure a proper coating of Fe_3O_4 nanoparticles on the sand particles, the coated sand was washed with distilled water until a clear supernatant was obtained. After washing the sand was filtered and dried at 85^oC for 3 hours. The Fe_3O_4 nanoparticles coated sand was stored in polyvinyl chloride (PVC) plastic bottles for further use.

4. Characterization of adsorbent

4.1. X-ray Diffraction (XRD)

To confirm the presence of Fe_3O_4 nanoparticles on the sand surface, X-ray Diffraction (XRD) was performed by using XRD 6000, Shimadzu analytical instrument**.**

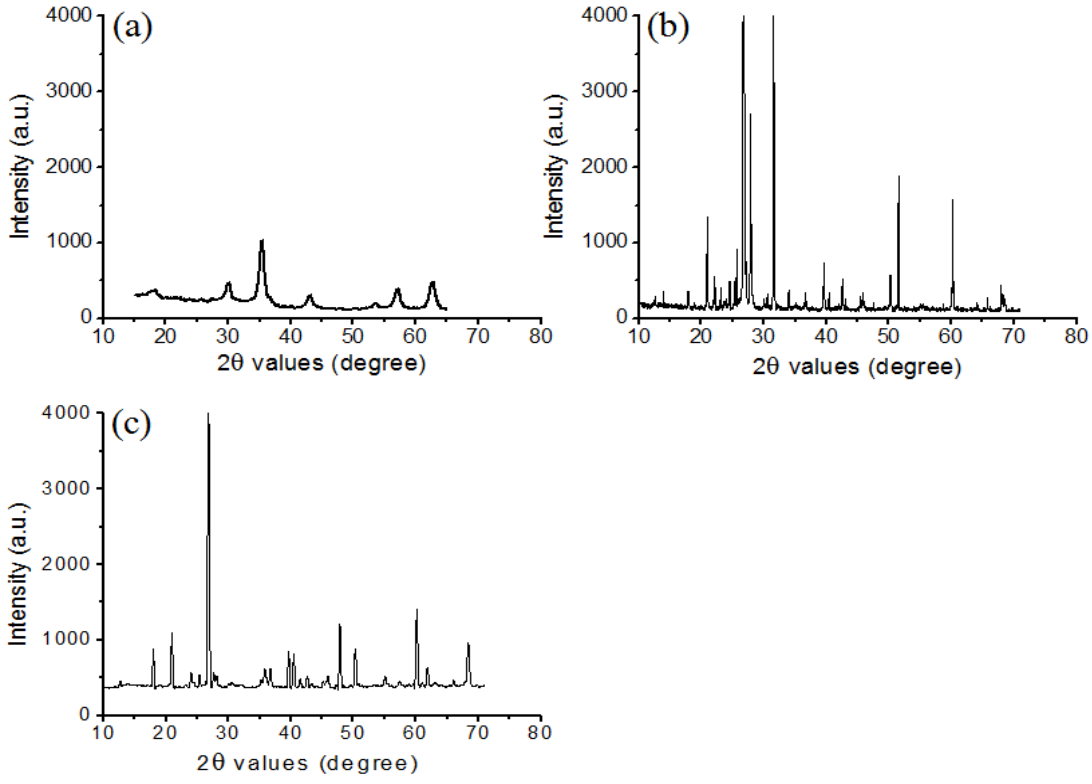

Fig. 1. XRD pattern of (a) Fe_3O_4 nanoparticles, (b) uncoated sand and (c) Fe_3O_4nanoparticles coated sand.

Fig. 1 shows powder XRD patterns of Fe_3O_4 nanoparticles (a), uncoated sand (b) and Fe_3O_4 nanoparticles coated sand (c). In fig. 1(a), characteristic peaks at $2\theta = 30.1^o$, 35.5^o, 43.06^o, 53.04^o, 57.3^o and 62.6^o are consistent with Fe_3O_4 as compared with JCPDS data (PDF No. 653107). In the XRD pattern of coated sand (fig. 1(c)) most of the peaks coincides with that of the pure Fe_3O_4 nanoparticles, indicating the formation of Fe_3O_4 nanoparticles on the sand surface. In case of the uncoated sand, sharp and narrow peaks are obtained at different positions which correspond to different faces present in sand and also indicate high crystallinity of the sand (fig. 1(b)). Some of the peaks in the XRD of coated sand i.e. at $2\theta = 18.058^o$, 20.89^o, 26.81^o, 40.43^o, 45.7^o, 50.01^o, 60.12^o and 68.33^o correspond to the peaks of uncoated sand.

4.2. Field Emission Scanning Electron Microscopy (FE-SEM)

The morphology of Fe_3O_4 nanoparticles was examined by Field Emission Scanning Electron Microscopy (FE-SEM), Hitachi S-4700.

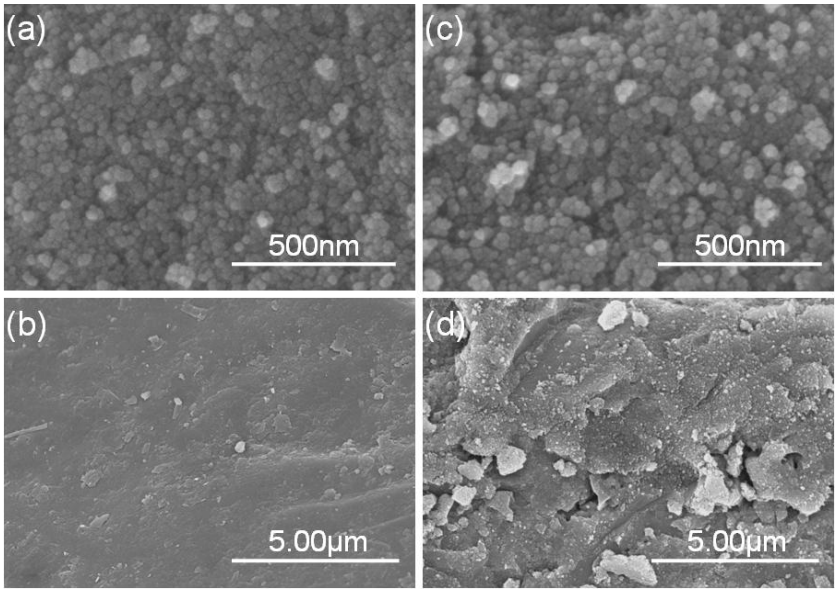

Fig. 2. FE-SEM images of (a) Fe_3O_4 nanoparticles, (b) uncoated sand, (c-d) Fe_3O_4 nanoparticles coated on sand surface

Fig. 2 shows FE-SEM images of: (a) Fe_3O_4 nanoparticles, (b) uncoated sand and (c-d) Fe_3O_4 nanoparticles coated sand. From the reaction solution, some un-attached Fe_3O_4 nanoparticles were also collected which are shown by FE-SEM image in fig. 2(a). The nanoparticles have size in the range of 20-60 nm. Fig. 2(b) shows bare sand particles; it shows that before coating the

surface of sand is clear, which after coating is covered with Fe_3O_4 nanoparticles of size 20-60 nm as shown in figs. 2(c), 2(d). FE-SEM images in figs. 2(a) and 2(c) indicates that the Fe_3O_4 nanoparticles have same morphology both in solution as well as on the sand surface.

5. Batch adsorption experiments

Batch adsorption experiments were performed to obtain rate and equilibrium data. In the batch adsorption experiments the parameters: contact time, initial pH of aqueous solution, adsorbent dose and initial As(III) concentration were varied. All the experiments were performed at room temperature in an incubator shaker at an agitation speed of 200 rpm. To study the effect of contact time on As(III) adsorption, the contact time was varied from 30 to 420 minutes, using 25g/L Fe_3O_4 coated sand adsorbent at initial As(III) concentration of 1mg/L and pH 7.0. The pH of the solution was varied from 2.0 to 12.0 for fixed adsorbent dose, contact time 420 minutes and initial As(III) concentrations of 1mg/L at room temperature. Study of the adsorbent dose was accomplished, by varying it from 5g/L to 30g/L and keeping other parameters fixed. In order to conduct isotherm studies, concentration of As(III) was varied from 3.5mg/L to 103.8mg/L for fixed values of adsorbent dose, contact time and pH. The batch experiments were also performed to study the effect of prominent background ions such as PO_4^{3-}, SO_4^{2-}, HCO_3^- and Cl^- on the As(III) removal efficiency. The concentration of these ions was varied from 5 to 100 mg/L while other parameters were kept fixed. Similar batch adsorption experiments were performed for As(V) removal. The solutions were filtered using 0.45µm durapore filter papers, acidified with 1% HNO_3 and finally analyzed for residual As(III) and As(V) concentration respectively using inductively coupled plasma mass spectrometer (ICP-MS).

As(III) or As(V) removal efficiency of Fe_3O_4 nanoparticles coated sand was calculated by using the formula:

$$\% \text{ As removal} = \frac{C_o - C_e}{C_o} \times 100 \qquad \text{(i)}$$

and the amount of As(III) or As(V) adsorbed (mg) per unit mass of adsorbent (g) i.e. q_e was determined by using the formula:

$$q_e = \frac{C_o - C_e}{M} \times V \qquad \text{(ii)}$$

where C_o and C_e are initial and final As(III) or As(V) concentrations (mg/L), respectively, V is the volume of solution in liters and M is the mass of the adsorbent in grams.

5.1. Results and discussion

5.1.1. Effect of contact time on As(III) and As(V) removal: adsorption kinetics

Fig. 3(a) and 3(b) shows the effect of contact time on %As(III) and %As(V) removal efficiency and adsorption capacity (q_t = mg/g) for initial As(III) and As(V) concentration of 1 mg/L respectively. From fig. 3(a) and 3(b), it can be seen that merely in 30 initial minutes of contact time, 82.84% of As(III) and 87% of As(V) are removed by Fe_3O_4 nanoparticles coated sand, whereas in next 330 minutes the removal efficiency of As(III) and As(V) reached to 99.6% and 99.84% respectively. Depending upon the %As(III) and %As(V) removal efficiency with respect to contact time, the whole removal process can be divided in two steps: fast and slower adsorption steps. In the fast adsorption step, the adsorbent has all its surface sites vacant for the adsorption and the As(III) or As(V) ions get easily adsorbed on these adsorption sites [15]. With the lapse of time, the available active sites are occupied by As(III) or As(V) and the process of adsorption gets slower and in about 360 minutes an equilibrium is attained as shown in the fig. 3(a) and 3(b). However, to ensure the complete adsorption all the batch experiments were performed for a contact time of 420 minutes.

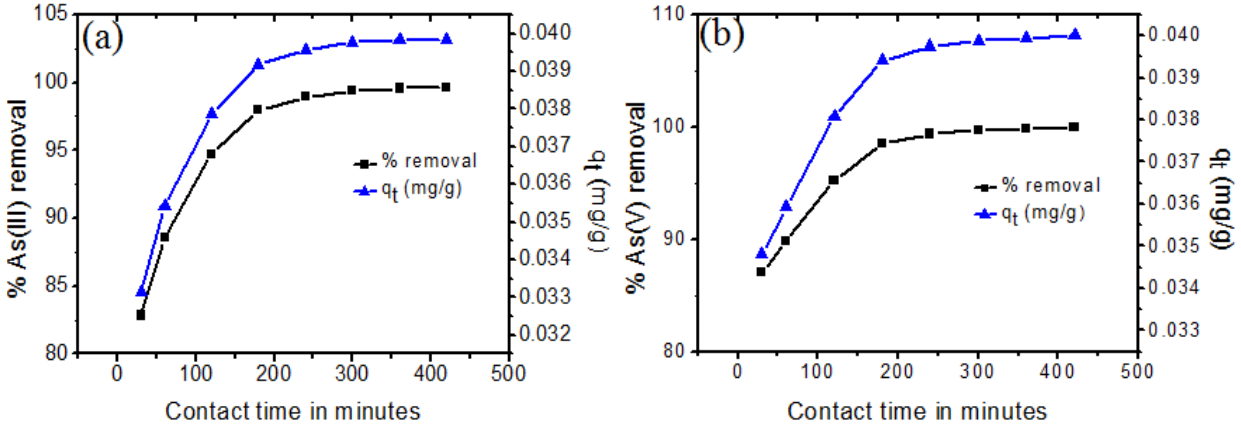

Fig. 3. Effect of contact time on % removal efficiency and adsorption capacity (q_t = mg/g) of (a) As(III) and (b) As(V)

In order to estimate the rate of adsorption and rate controlling step, pseudo-first order and pseudo-second-order kinetics model were employed. The following equation (iii) represent pseudo-first order kinetics model [16]

$$\log(q_e - q_t) = \log q_e - \frac{k_{ads}}{2.303} t \qquad \text{(iii)}$$

where q_e (mg/g) and q_t (mg/g) are amount of As(III) or As(V) adsorbed per unit mass of adsorbent at equilibrium and time t, respectively. The k_{ads} is the pseudo-first order rate constant, which can be obtained from slope of linear plot log (q_e-q_t) vs time (t).

Similarly, equation (iv) represent pseudo-second-order kinetics model [17]

$$\frac{t}{q_t} = \frac{1}{h} + \frac{t}{q_e} \qquad \text{(iv)}$$

and

$$h = kq_e^2 \qquad \text{(v)}$$

where q_e (mg/g) and q_t (mg/g) are amount of As(III) or As(V) adsorbed per unit mass of adsorbent at equilibrium and time t, respectively. The k is the pseudo-second-order adsorption rate constant and h is the initial adsorption rate (mg g^{-1} min^{-1}). The values of q_e (1/slope), k (slope^2/intercept) and h (1/intercept) can be calculated from the plots of t/q_t vs t. The plots of pseudo-first order and pseudo-second-order kinetics model for As(III) are shown in figs. 4(a) and 4(b) and for As(V) are shown in figs. 5(a) and 5(b) respectively. The values of various corresponding parameters; k_{ads}, k, h and correlation coefficients R^2 obtained from these plots are shown in Table 1. The experimental kinetics data of both As(III) and As(V) fitted well in pseudo-second-order kinetics model with higher correlation coefficients (R^2 = 0.999) as compared with pseudo-first-order kinetics model which has lower correlation coefficients. The experimental values of q_e i.e. 0.0398 in case of As(III) and 0.0399 in case of As(V) are more close to theoretical q_e values i.e. 0.040 for As(III) and 0.0406 for As(V) respectively obtained from pseudo-second-order model in comparison to 0.015 and 0.009 q_e values obtained from pseudo-first-order-model. This also support that data is fitted well in pseudo-second-order kinetics model. These results reveal that adsorption process is chemisorption i.e. there is some chemical bonding between adsorbent and adsorbate [18].

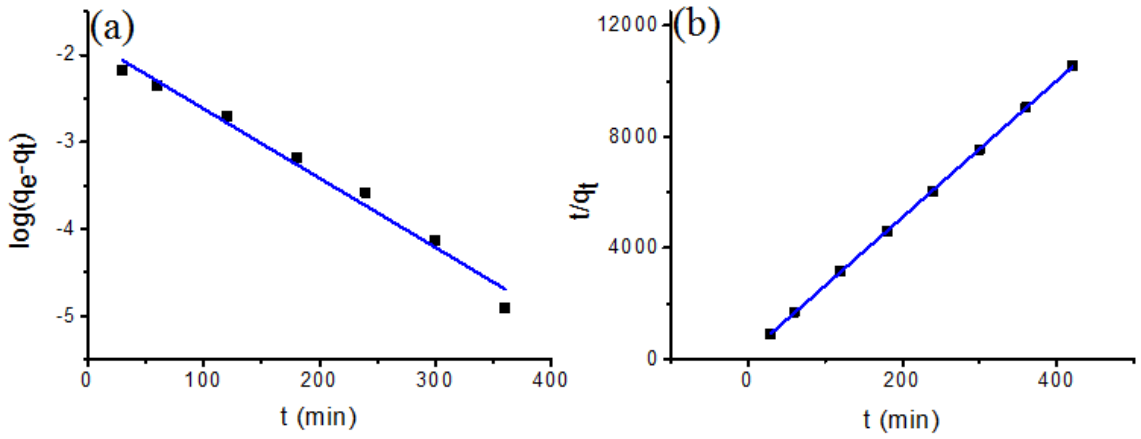

Fig. 4. Adsorption kinetics (a) pseudo-first-order model and (b) pseudo-second-order model for As(III) removal by Fe_3O_4 nanoparticles coated sand.

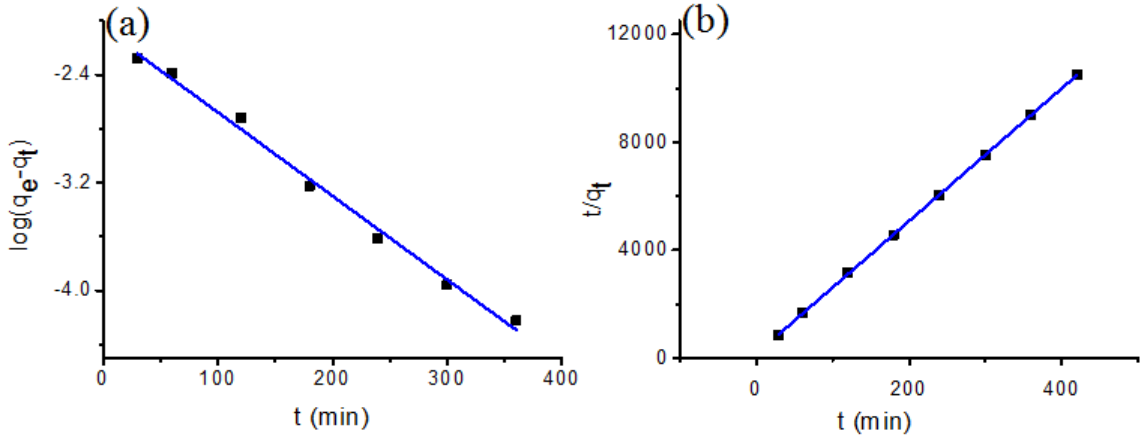

Fig. 5. Adsorption kinetics (a) pseudo-first-order and (b) pseudo-second-order model for As(V) removal by Fe_3O_4 nanoparticles coated sand.

Table 1: Pseudo-first-order and pseudo-second-order kinetic model parameters for As(III) and As(V) adsorption by Fe_3O_4 nanoparticles coated sand.

Arsenic species	**Pseudo-first-order parameters**			**Pseudo-second-order parameters**				**Experimental**
	k_{ads} (min^{-1})	R^2	q_e (mg/g)	k (g mg^{-1} min^{-1})	h (mg g^{-1} min^{-1})	q_e (mg/g)	R^2	q_e (mg/g)
As(III)	0.0183	0.978	0.015	3.21	0.0053	0.040	0.999	0.0398
As(V)	0.0142	0.992	0.009	3.75	0.0062	0.0406	0.999	0.0399

5.1.2. Effect of initial solution pH on As(III) and As(V) removal

The pH of water is considered an important factor in the adsorption based wastewater treatment experiments as it affects metal speciation in the water. Fig. 6(a) and 6(b) shows the effect of water pH on the removal efficiency of As(III) and As(V) respectively by Fe_3O_4 nanoparticles coated sand. The effect of pH can be explained in terms of point of zero charge(pHz) of the adsorbent (pHz of adsorbent is nearly 7.8) at which the surface of the adsorbent is neutral. From fig. 6, it can be seen that with an increase in the pH of water from 2.0 to 8.0, As(III) removal efficiency increases from 98.92% to 99.63%, This is due to the fact that below pHz (7.8) the surface of adsorbent Fe_3O_4 is positively charged, and As(III) exists in non-ionic (H_3AsO_3) state in the low pH (2.0 to 6.0) range. Therefore, when non-ionic As(III) species comes in contact with Fe_3O_4 its positively charged surface helps non-ionic As(III) to convert into anionic one, which in turn assists adsorption process [19]. At pH values 6.5 to 8.0 the neutral As(III) ions dissociates and produces anionic $H_2AsO_3^-$ and $HAsO_3^{2-}$ ions which are attracted to positively charged surface (below pH 7.8) of adsorbent resulting in high As(III) removal.

Even in the pH range from 8.0 to12.0, As(III) remains in anionic state but above pHz (7.8) the adsorbent surface become negatively charged. Therefore in this pH range, the decreasing As(III) uptake from 99.63% to 62.8% are due the following reasons: (i) the competition of excessive OH^- ions for adsorption, (ii) domination of negatively charged sites on Fe_3O_4 nanoparticles coated sand and (iii) domination of negatively charged As(III) species ($H_2AsO_3^-$). With increasing pH, there is a gradual increase in the repulsive forces between negatively charged Fe_3O_4 nanoparticles coated sand and the negatively charged As(III) ions, which results in a decreasing As(III) removal efficiency.

In case of As(V), it is observed that for the pH range 2.0-7.0 there is slight decrease in As(V) removal efficiency, while for the increased pH from 7.0 to 12.0, there is a drastic decrease in As(V) removal efficiency from 99.99% to 39.33%. It indicates that Fe_3O_4 nanoparticles coated sand adsorb As(V) more efficiently in an acidic pH range than in basic pH range. The observed variation in As(V) removal efficiency at different pH values may be attributed to different affinities of Fe_3O_4 nanoparticles coated sand for different As(V) species viz. AsO_4^{3-}, $HAsO_4^{2-}$, $H_2AsO_4^-$, H_3AsO_4 dominating at different pH values. We know that most of the groundwater

exists in the pH range from 7.0 to 7.5 and therefore in this study we have analyzed batch experiments at most natural pH '7.0'.

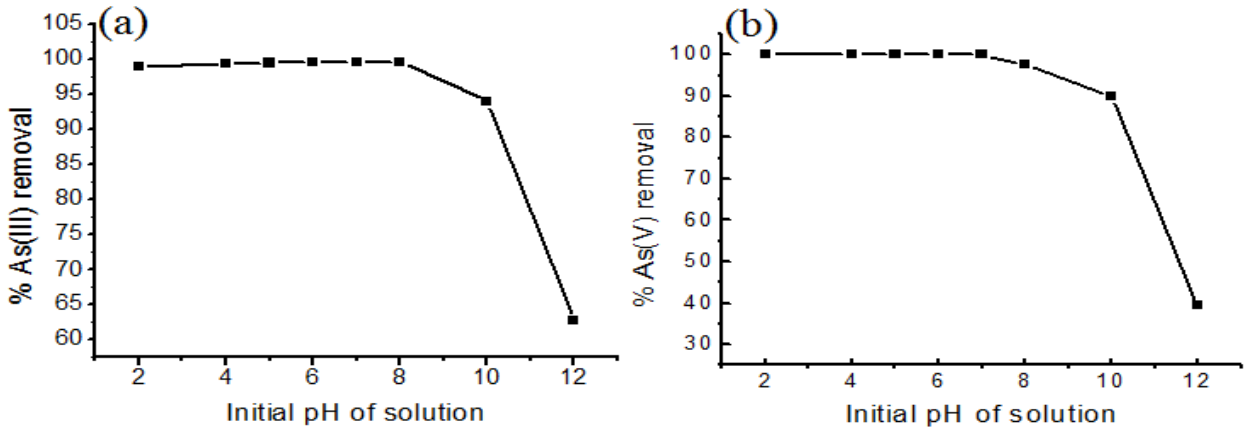

Fig. 6. Effect of pH on (a) As(III) removal efficiency and (b) As(V) removal efficiency

5.1.3. Effect of adsorbent dose on As(III) and As(V) removal

Fig. 7(a) and 7(b) shows the effect of adsorbent dose on %As(III) and %As(V) removal efficiency and adsorption capacity at fixed initial As(III) or As(V) concentration of 1mg/L respectively, and pH 7.0. It was observed that with an increase in adsorbent dose from 5g/L to 30g/L, the As(III) removal efficiency increased from 88.93% to 99.89% and As(V) removal efficiency increased from 94.7% to 99.99% which is due to available more active sites at higher concentrations of the adsorbent. However, beyond 25g/L dose, no significant change in As(III) or As(V) removal efficiency was observed. On the other hand the As(III) adsorption capacity decreased from 0.178 mg/g to 0.0333 mg/g and As(V) adsorption capacity decreased from 0.189 mg/g to 0.033 mg/g. This decrease is due to the interference between binding sites, and higher adsorbent dose or inadequate number of As ions in the solution with respect to available binding sites [20]. In both plots, the point of intersection (fig. 7(a) and 7(b)) is usually considered as the optimum dose that represents balance between %As(III) or %As(V) removal efficiency and adsorption capacity respectively. In our case, the point of intersection is approximately at 10 g/L of adsorbent dose, but this dose was not able to reduce As(III) or As(V) concentration below 10 µg/L value i.e. the MCL value set by WHO. Therefore, a dose of 25 g/L, at which As level dropped below the MCL value, was selected for further analysis. However, in this study it should

be noted that the dose of real adsorbent (Fe_3O_4 nanoparticles) might be much lesser than the weighted dose because it was coated on bulky sand particles, the weighted dose is actually the contribution of both real adsorbent Fe_3O_4 nanoparticles and sand.

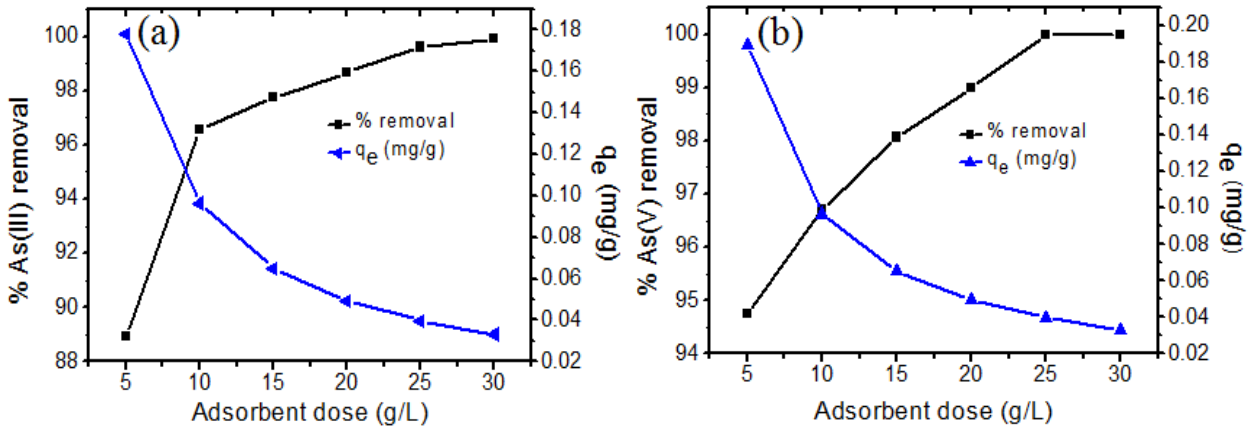

Fig. 7. Effect of adsorbent dose on % removal efficiency and adsorption capacity (q_e = mg/g) of (a) As(III) and (b) As(V)

5.1.4. Effect of initial As(III) or As(V) concentration

Fig. 8(a) and 8(b) shows the effect of initial As(III) or As(V) concentration on the removal efficiency and adsorption capacity of Fe_3O_4 nanoparticles coated sand. It is observed that with the increase in initial As(III) or As(V) concentration the As(III) or As(V) removal efficiency decreases while the adsorption capacity increases and became saturated approximately at 80mg/L of both As(III) or As(V) concentration. This is because at lower As(III) or As(V) concentration, the number of adsorbent surface active sites are sufficiently large and accommodates abundant of As(III) or As(V) ions. An increase in the As(III) or As(V) concentration causes a reduction in the proportion of surface active sites to As(III) or As(V) ions. Thus an insufficient accommodation of As(III) or As(V) ions results in the decreasing %As(III) or %As(V) removal efficiency. Furthermore a driving force is provided by initial As(III) or As(V) concentration to overcome all mass transfer resistances between the adsorbent and adsorption medium which results in higher adsorption capacities at higher initial As(III) or As(V) concentration [20].

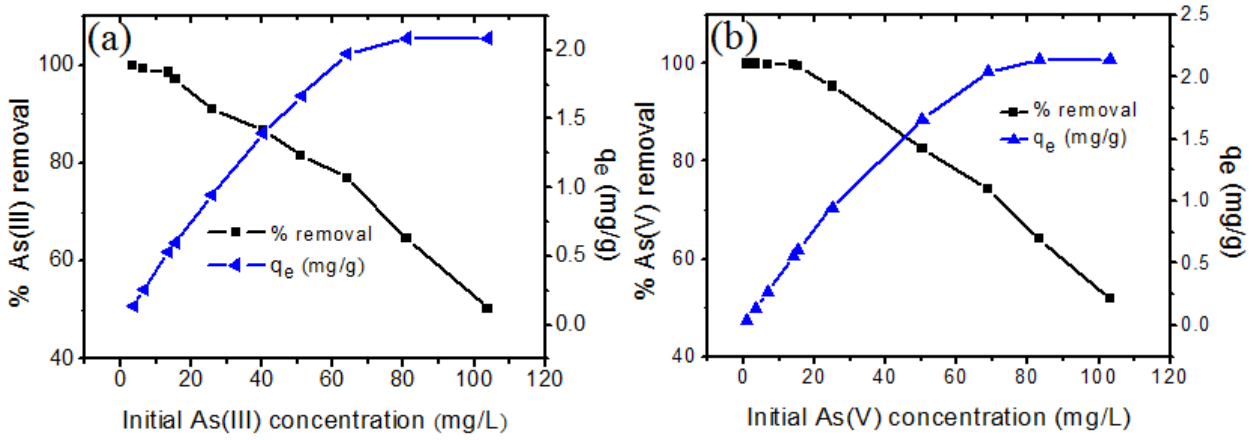

Fig. 8. Effect of (a) initial As(III) concentration on % As(III) removal efficiency and adsorption capacity (q_e = mg/g) and (b) initial As(V) concentration on % As(V) removal efficiency and adsorption capacity (q_e = mg/g)

5.1.5. Adsorption isotherms

We know that the adsorption isotherm gives an idea about the interaction between adsorbate and adsorbent in an adsorption system. Therefore, in order to study the adsorbate-adsorbent interaction and to compute various adsorption parameters, we have used Freundlich and Langmuir isotherm models to fit the experimental adsorption equilibrium data of As(III) or As(V) removal by Fe_3O_4 nanoparticles coated.

The Freundlich isotherm in linear form is represented as [21]

$$\log(q_e) = \log K_F + \frac{1}{n}\log(C_e) \qquad \text{(vi)}$$

where C_e is the equilibrium concentration of As(III) or As(V) in the solution phase (mg/L), q_e is the amount of As(III) or As(V) adsorbed onto the Fe_3O_4 nanoparticles coated sand at equilibrium (mg/g), K_F is adsorption capacity indicator and n (which lies between 1 to 10) is the heterogeneity factor indicating favorable adsorption. It is reported that if the value of n lies between 2 to 10 the adsorption is considered as better adsorption, and if it lies between 1 to 2 the adsorption is considered to be good.

Linear form of Langmuir isotherm model can be written as [22]

$$\frac{C_e}{q_e} = \frac{C_e}{q_m} + bq_m \qquad \text{(vii)}$$

where C_e is the As(III) or As(V) concentration in the solution and q_e is the As(III) or As(V) amount adsorbed at equilibrium. The q_m(mg/g) is the saturated monolayer adsorption capacity, and b (L/mg) is the Langmuir constant related to the affinity between solute and adsorbent.

A dimensionless quantity 'r' was also calculated in order to predict the adsorption efficiency of the isotherm process by using following equation.

$$r = \frac{1}{1 + bC_0} \qquad \text{(viii)}$$

where C_0 is the initial concentration of As(III) or As(V) and b is Langmuir constant. The value of 'r' defines the shape of the isotherm. The value $0 < r < 1.0$ represents favourable Langmuir isotherm adsorption, whereas $r = 0$ represents irreversible adsorption, $r = 1$ shows linear adsorption and $r > 1.0$ represents unfavourable adsorption.

Linearized Freundlich and Langmuir adsorption isotherm plots of As(III) and As(V) removal are shown in figs. 9(a) and 9(b); and 10(a) and 10(b), respectively. Values corresponding to various parameters of Langmuir and Freundlich isotherms are listed in Table 2.

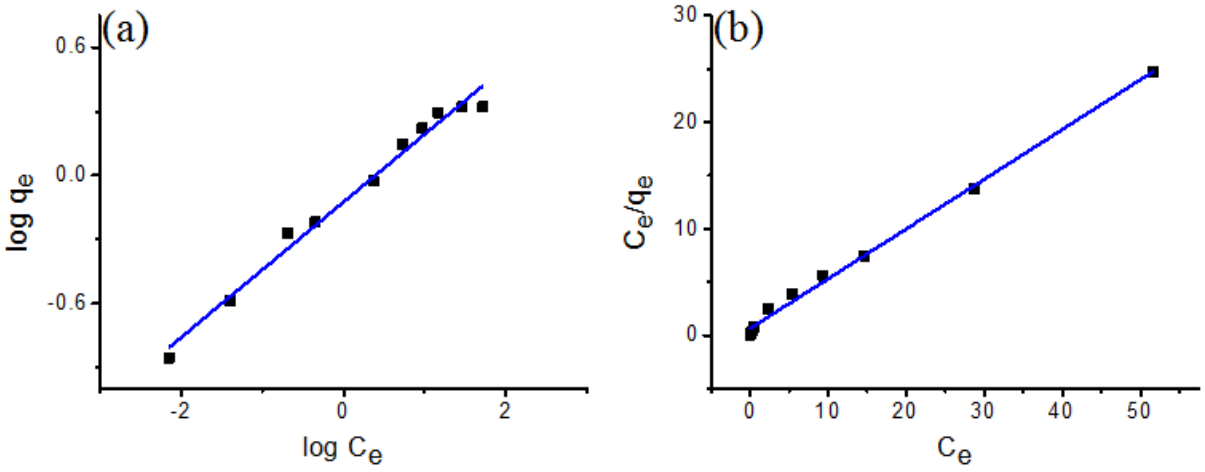

Fig. 9. Adsorption isotherm (a) Freundlich fit and (b) Langmuir fit for As(III) adsorption by Fe_3O_4 nanoparticles coated sand.

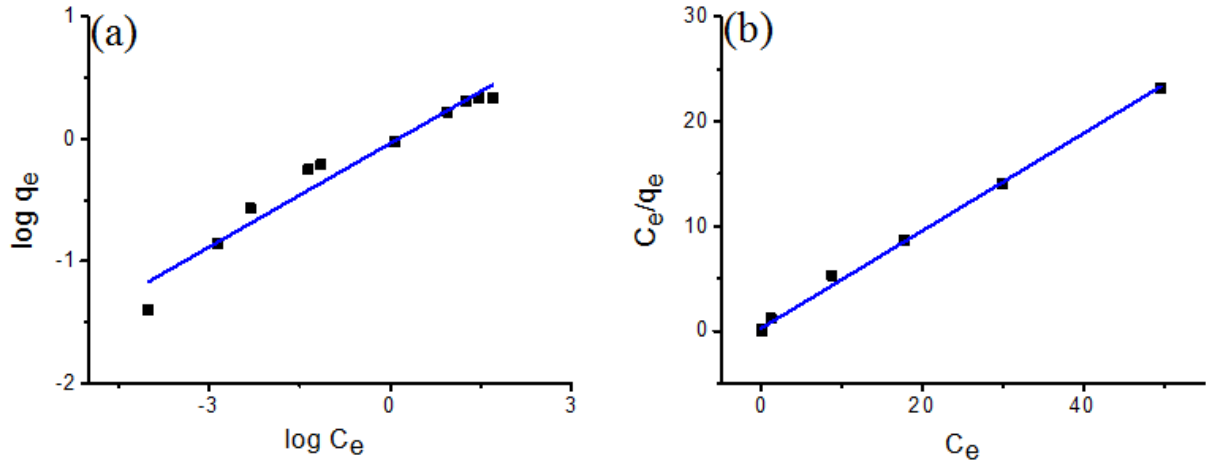

Fig. 10. Adsorption isotherm (a) Freundlich fit and (b) Langmuir fit for As(V) adsorption by Fe_3O_4 nanoparticles coated sand.

Table 2: Freundlich and Langmuir adsorption isotherm parameters for As(III) and As(V) adsorption by Fe_3O_4 nanoparticles coated sand.

Arsenic species	**Freundlich isotherm parameters**			**Langmuir isotherm parameters**			
	K_F (mg/g)	n	R^2	b (L/mg)	q_m(mg/g)	r	R^2
As(III)	0.75	3.15	0.983	0.709	2.14	0.287-0.013	0.996
As(V)	0.9203	3.54	0.951	1.686	2.15	0.372-0.0057	0.997

In our case the calculated value of n for As(III) is 3.15 and for As(V) is 3.54, which lies between the limit for better adsorption i.e. $2 < n < 10$. The obtained higher correlation coefficient ($R^2 > 0.99$) for both As(III) and As(V) while using Langmuir model indicates that the experimental data are better fitted by Langmuir model as compared with Freundlich model where R^2 is smaller than the previous one. This interprets monolayer adsorption of As(III) and As(V) on a homogeneous surface. Here, the maximum adsorption capacity (q_m) for As(III) and As(V) removal is obtained 2.14 mg/g and 2.15 mg/g respectively. The values of r are obtained to be less than unity with a decreasing order at high As(III) and As(V) concentrations, which indicates highly favorable adsorption of As(III) or As(V) on Fe_3O_4 nanoparticles coated sand.

5.1.6. Effect of background ions on As(III) and As(V) removal efficiency

The effect of PO_4^{3-}, SO_4^{2-}, HCO_3^- and Cl^- ions on As(III) and As(V) removal efficiency was also studied because these are commonly present in the water environment which may interfere adsorption process. Fig. 11(a) and (b) shows the results for individual effects of various background ions (PO_4^{3-}, SO_4^{2-}, HCO_3^- and Cl^-) on %As(III) and %As(V) removal efficiency by Fe_3O_4 nanoparticles coated sand respectively.

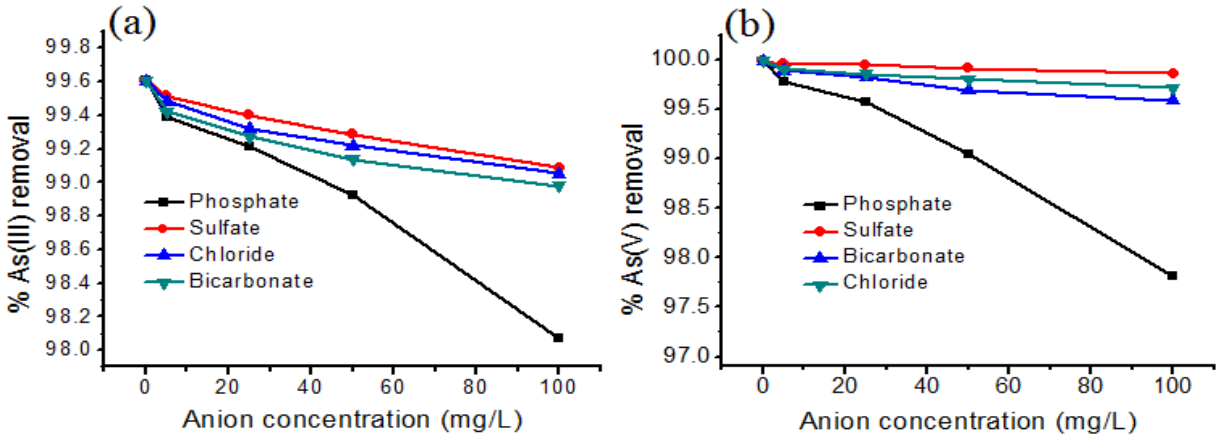

Fig. 11. Effect of co-existing anions on (a) As(III) removal efficiency and (b) As(V) removal efficiency

It is observed that the presence of sulphate has a negligible effect on both As(III) and As(V) removal efficiency, whereas the other ions Cl^-, HCO_3^-, PO_4^{3-} have an influence but still minute on As(III) and As(V) removal in their concentration range of 5 mg/L to 100 mg/L.

The results of this study show that the presence of background ions effects the As(III) and As(V) removal efficiency in the order of $PO_4^{3-} > HCO_3^- > Cl^- > SO_4^{2-}$, however this effect is very small.

6. Thermodynamic investigation of As(III) and As(V) removal by Fe_3O_4 nanoparticles coated sand

We have also conducted arsenic removal experiments at different temperatures to evaluate the feasibility and nature of the adsorption process. The various thermodynamic parameters associated with adsorption i.e. Gibbs free energy change (ΔG^o), enthalpy change (ΔH^o) and entropy change (ΔS^o) were calculated as follows:

$$\Delta G^\circ = -RTlnK_L \qquad \text{(ix)}$$

Where ΔG^o is Gibbs free energy change of adsorption in kJ/mol, T is the temperature in Kelvin, R is the gas constant having a value of 8.314 J/mol K, and K_L is the equilibrium constant obtained from Langmuir model.

Acc. to thermodynamics, the Gibbs free energy change is also related to the enthalpy change (ΔH^o) and entropy change (ΔS^o) at constant temperature by eq. (x)

$$\Delta G^\circ = \Delta H^\circ - T\Delta S^\circ \qquad \text{(x)}$$

Now using eqs. (ix) and(x) we have eq. (xi)

$$lnK_L = \frac{\Delta S^\circ}{R} - \frac{\Delta H^\circ}{RT} \qquad \text{(xi)}$$

The values of enthalpy change (ΔH^o) and entropy change (ΔS^o) were calculated from the slope and intercept of the plot of $\ln K_L$ versus $1/T$ (Fig. 12(a) and 12(b)) and are listed in table 3. It can be seen that ΔG^o values for both As(III) and As(V) were found to be negative for all temperature conditions studied, indicating that the adsorption process is spontaneous in nature. The values of enthalpy change (ΔH^o) and entropy change (ΔS^o) comes out to be positive. The positive values of ΔH^o indicate that the adsorption process is endothermic in nature. The positive values of ΔS^o suggests an increase in degree of randomness at the solid-liquid interface during the adsorption of As(III) and As(V) on Fe_3O_4 nanoparticles coated sand.

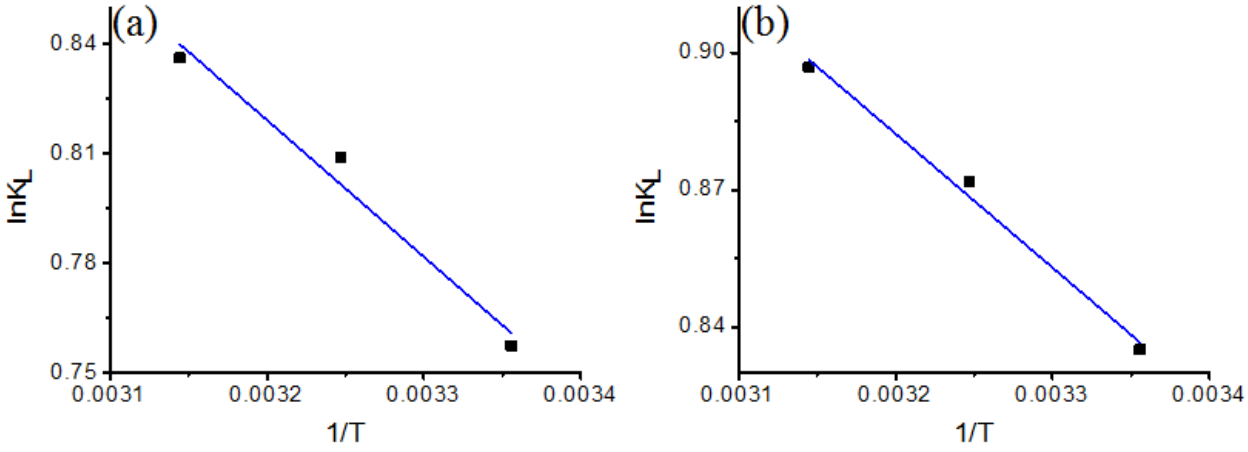

Fig. 12. Plot of $\ln K_L$ vs 1/T for determination of thermodynamic parameters for (a) As(III) and (b) As(V) removal

Table 3: Thermodynamic parameters obtained from $\ln k_L$ vs 1/T plot for As(III) and As(V) removal

Arsenic species	**Thermodynamics parameters**					**K_L (L/g) At different temperature**		
	ΔH^o (kJ/mol)	ΔS^o (J/mol)	ΔG^o (J/mol) At different temperature					
			298 K	308 K	318 K	298 K	308 K	318 K
As(III)	3.108	16.757	-1876.49	-2071.32	-2210.42	2.133	2.245	2.308
As(V)	2.436	15.132	-2069.08	-2232.63	-2371.17	2.305	2.391	2.452

7. Column adsorption experiments

A fixed bed column study was conducted by using an ordinary 100 mL burette made of borosilicate glass with an internal diameter of 2 cm and 55 cm height. The effect of bed height on breakthrough curve was studied by varying the bed height from 5 cm to 10 cm. The bottoms of the columns were plugged in with glass wool just to make a support for the Fe_3O_4 nanoparticles coated sand to prevent it floating from the outlet. The columns were packed with the desired amount of Fe_3O_4 nanoparticles coated sand to the required height. The column was then operated in such-manner that a calculated amount of As(III) solution of 1mg/L concentration was constantly added to it through a graduated cylinder and allowing it to flow along gravity in down flow mode with a constant rate. The rate of flow was constantly checked by measuring the amount flowing per minute at regular intervals of time. Once the column was started, the samples were collected at certain time intervals using reagent bottles. This process was continued until the column gets exhausted and the amount of arsenic in different samples was then analyzed for residual arsenic concentrations.

Similar columns were run for As(V) removal by varying the bed height (5 cm and 10 cm). All the columns were run at room temperature at neutral pH 7.0. Fig. 13. represent schematic of experimental setup used for column studies of arsenic removal.

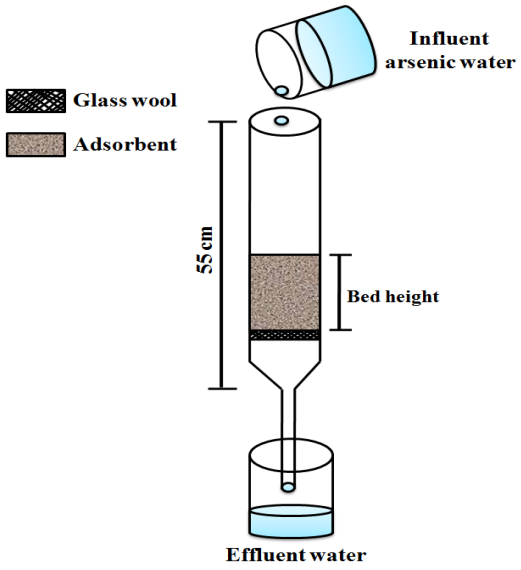

Fig. 13. Schematic of experimental setup for column studies of arsenic removal

The breakthrough time was taken when As(III) or As(V) concentration in the effluent exceeds maximum contaminant limit i.e. 10 µg/L and the column was considered exhausted when arsenic concentration in effluent exceeds 50% of influent arsenic concentration. The breakthrough time and exhaustion time for As(III) and As(V) at different bed heights is shown in table 4. It has been found that breakthrough time and exhaustion time for As(V) is greater than As(III).

Table 4: Effect of bed height on the column breakthrough and exhaustion time

Arsenic species	**Breakthrough time (hr) at different bed height**		**Exhaustion time (hr) at different bed height**	
	5 cm	10 cm	5 cm	10 cm
As(III)	6 hrs	17 hrs	21 hrs	56 hrs
As(V)	7 hrs	17 hrs	30 hrs	59 hrs

8. Summary

The Fe_3O_4 nanoparticles coated sand has been successfully synthesized and characterized by using XRD and SEM technique. The synthesized adsorbent has been used for As(III) and As(V) removal from aqueous solution. Batch kinetic study shows that the equilibrium is reached within 360 minutes of contact time and the experimental kinetics data for both As(III) and As(V) fitted

well in pseudo-second order kinetics model with high correlation coefficients as compared to pseudo-first-order kinetics model. The batch adsorption isotherm data is well fitted in Langmuir adsorption isotherm with higher correlation coefficients, indicating monolayer adsorption of As(III) or As(V) on the surface of adsorbent. The maximum Langmuir capacity for As(III) and As(V) sorption is found to be 2.14 mg/g and 2.15 mg/g respectively. The obtained adsorbent shows a significant 99.6% removal of As(III) and 99.99% removal of As(V) in most natural conditions. The thermodynamic studies show that ΔG^o is negative at all studied temperature conditions which indicate that the arsenic removal is spontaneous in nature. We have also performed column studies for As(III) and As(V) removal and found higher breakthrough and exhaustion time for As(V) removal as compared to As(III) removal. Since Fe_3O_4 coated sand shows high adsorption capacity and affinity towards both As(III) and As(V), therefore, by utilizing the Fe_3O_4 coated sand the problem of extraction of nanoparticles from treated water can be overcome by removing the adsorbent by a simple filtration process. The nano adsorbent coated sand provides an economically feasible solution for common man for As(III) and As(V) removal from drinking water.

References:

[1] Kanel S. R., Manning B., Charlet L., & Choi H., *"Removal of arsenic (III) from groundwater by Nanoscale zero-valent iron"* Environmental and Science Technology, vol. 39(5), pp. 1291-1298, January 2005.

[2] Malana M. A., Qureshi R. B., & Ashiq M. N., "*Adsorption studies of arsenic on nano aluminium doped manganese copper ferrite polymer (MA, VA, AA) composite: kinetics and mechanism*" Chemical Engineering Journal, vol. 172(2-3), pp. 721–727, August 2011.

[3] Smith A.H., Lingas E.O., & Rahman M., "*Contamination of drinking-water by arsenic in Bangladesh: a public health emergency*" Bulletin of the World Health Organization, vol. 78(9), pp. 1093–1103, January 2000.

[4] Souter P. F., Cruickshank G. D., Tankerville M. Z., Keswick B. H., Ellis B. D., Langworthy D. E., Metz K. A., Appleby M. R., Hamilton N., Jones A. L., & Perry J. D., "*Evaluation of a new water treatment for point-of-use house-hold applications to remove microorganisms and arsenic from drinking water*" Journal of Water and Health, Vol. 1(2), pp. 73-84, June 2003.

[5] Bagla P., & Kaiser J., "*India's spreading health crisis draws global arsenic experts*" Science, vol. 274(5285), pp. 174-175, October 1996.

[6] Chakraborti A. K., & Saha K. C., "*Arsenical dermatosis from tube well water in West Bengal*" Indian Journal of Medical Research, vol. 85, pp. 326-334, March 1987.

[7] Pena M. E., Meng X. G., Korfiatis G. P. & Jing C. Y., "*Adsorption mechanism of arsenic on nanocrystalline titanium dioxide*" Environmental Science and Technology, vol. 40(4), pp. 1257–1262, February 2006.

[8] Kundu S., & Gupta A. K., "*As(III) removal from aqueous medium in fixed bed using iron oxide-coated cement (IOCC): experimental and modeling studies*" Chemical Engineering Journal, vol. 129(1-3), pp. 123–131, May 2007.

[9] Sarkar S., Gupta A., Biswas R. K., Deb A. K., Greenleaf J. E., & Sen Gupta A. K., "*Well head arsenic removal units in remote villages in Indian Subcontinent: field results and performance evaluation*" Water Research, vol. 39(10), pp. 2196–2206, May 2005.

[10] Shipley H. J., Yean S., Kan A. T., & Tomson M. B., "*Adsorption of arsenic to magnetite nanoparticles: effect of particle concentration, pH, ionic strength, and temperature*" Environmental Toxicology and Chemistry, vol. 28(3), pp. 509-515, March 2009.

[11] Wang C., Luo H., Zhang Z., Wu Y., Zhang J., & Chen S., "*Removal of As(III) and As(V) from aqueous solutions using nanoscale zero valent iron-reduced graphite oxide modified composites*" Journal of Hazardous Materials, vol. 268, pp. 124–131, March 2014.

[12] Jessen S., Larsen F., Koch C. B., & Avin E., "*Sorption and desorption of arsenic to ferrihydrite in a sand filter*" Environmental Science and Technology, vol. 39(20), pp. 8045-8051, September 2005.

[13] Guo H. M., Stuben D., & Berner Z., "*Adsorption of arsenic (III) and arsenic(V) from groundwater using natural siderite as the adsorbent*" Journal of Colloid and Interface Science, vol. 315(1), pp. 47-53, November 2007.

[14] An B., Liang Q., & Zhao D., "*Removal of arsenic (V) from spent ion exchange brine using a new class of starch-bridged magnetite nanoparticles*" Water Research, vol. 45(5), pp. 1961-1972, 2011.

[15] Chowdhury S. R., & Yanful E. K., "*Arsenic and chromium removal by mixed magnetite-maghemite nanoparticles and the effect of phosphate on removal*" Journal of Environmental Management, vol. 91(11), pp. 2238-2247, November 2010.

[16] Lagergren S., "*About the theory of so-called adsorption of soluble substance*" Kungliga Svenska Vetenskapsakademiens Handlingar, vol. 24, pp. 1–39, 1898.

[17] Ho Y. S., & McKay G., "Kinetic models for the sorption of dye from aqueous solution by wood" Journal of Environmental Science and Health Part B: Process Safety Environmental Protection, vol. 76(2), pp. 183–191, May 1998.

[18] Ren Z., Zhang G., & Chen J. P., "*Adsorptive removal of arsenic from water by an iron-zirconium binary oxide adsorbent*" Journal of Colloid and Interface Science, vol. 358(1), pp. 230-237, June 2011.

[19] Gupta A., Mohammed Y., & Sankararmakrishnan N., "*Chitosan- and Iron- chitosan-coated sand filters: A cost-effective approach for enhanced arsenic removal*" Industrial and Engineering Chemistry Research, vol. 52(5), pp. 2066-2072, January 2013.

[20] Fan T., Liu Y., Feng B., Zeng G., Yang C., Zhou M., Zhou H., Tan Z., & Wang X., "*Biosorption of cadmium(II), zinc(II) and lead(II) by Penicillium simplicissimum: isotherms, kinetics and thermodynamics*" Journal of Hazardous Materials, vol. 160(2-3), pp. 655–661, December 2008.

[21] Freundlich H. M. F. Z., "*Stoechiometrie und Verwandtschaftslehre*" Zeitschriftfuer Physikalische Chemie, vol. 57, pp. 385-470, 1906.

[22] Wang X., Guo Y., Yang L., Han M., Zhao J., & Cheng X., "*Nanomaterials as sorbents to remove heavy metal ions in wastewater treatment*" Journal of Environmental and Analytical Toxicology, vol. 2(7), pp. 154(1)-154(7), August 2012.

List of Publications

Journal Publications

1. **Sarita Kango**, Rajesh Kumar, (2016) "Low-cost magnetic adsorbent for As(III) removal from water: adsorption kinetics and isotherms", Environmental Monitoring and Assessment, 188:60(1)-60(14).

2. **Sarita Kango**, Rajesh Kumar, (2016) "Magnetite nanoparticles coated sand for arsenic removal from drinking water", Environmental Earth Sciences (accepted).

Conference Proceeding

1. **Sarita Kango**, Rajesh Kumar, (2015) "Magnetite nanoparticles coated glass wool for As(V) removal from drinking water", AIP Conference Proceeding, 1675:0300241-0300244.

Book Chapter

1. **Sarita Kango,** Rajesh Kumar, (2015) **"**Efficient removal of arsenic (III) from drinking water by Fe_3O_4 nanoparticles coated sand: Time dependent removal study", In: Nanotechnology: Novel Perspectives and Prospects (pp.), Publisher: Tata-McGraw Hill, New Delhi (India), Editors: Bhupinder Singh, Anupama Kaushik, S. K. Meheta, S. K. Tripathi.

Poster Presentations in Conferences

1. **Sarita Kango,** Rajesh Kumar, "Synthesis and characterization of magnetic adsorbent for arsenite removal from aqueous solution", Presented in 2nd National Conference on Multifunctional Advanced Materials (MAM-2014) held on 11-13 June, 2014 at Shoolini University, Solan, Himachal Pradesh, India.

2. **Sarita Kango**, Rajesh Kumar, "Kinetics study of As(III) removal from drinking water by magnetic adsorbent coated on glass wool", 2nd International Convention of Engineering and Management (ICEM) held on 4-5 April 2015 at JUIT Waknaghat, Solan, India.